SEM/EDS investigation of one-step flame sprayed and fused Ni-based self-fluxing alloy coatings on steel substrates

Šimunovic, Katica; Slokar, Ljerka; Havrlišan, Sara

Philosophical Magazine

ISSN: 1478-6435 (Print) 1478-6443 (Online) Journal homepage: www.tandfonline.com/journals/tphm20

SEM/EDS investigation of one-step flame sprayed and fused Ni-based self-fluxing alloy coatings on steel substrates

Katica Simunovic, Ljerka Slokar & Sara Havrlisan

To cite this article: Katica Simunovic, Ljerka Slokar & Sara Havrlisan (2017) SEM/EDS investigation of one-step flame sprayed and fused Ni-based self-fluxing alloy coatings on steel substrates, Philosophical Magazine, 97:4, 248-268, DOI: 10.1080/14786435.2016.1257167

To link to this article: https://doi.org/10.1080/14786435.2016.1257167

PHILOSOPHICAL MAGAZINE, 2017
VOL. 97, NO. 4, 248–268
http://dx.doi.org/10.1080/14786435.2016.1257167

Taylor & Francis
Taylor & Francis Group

SEM/EDS investigation of one-step flame sprayed and fused Ni-based self-fluxing alloy coatings on steel substrates

Katica Simunovic[a], Ljerka Slokar[b] and Sara Havrlisan[a]

[a]Mechanical Engineering Faculty in Slavonski Brod, University of Osijek, Slavonski Brod, Croatia; [b]Faculty of Metallurgy, University of Zagreb, Sisak, Croatia

ABSTRACT

This study presents the results of light optical and scanning electron microscopy as well as energy dispersive spectroscopy investigation of the Ni-based self-fluxing alloys (NiCrBSi, NiCrWBSi and NiCrBSi + WC) deposited on steel substrates (heat treated carbon steel C45, heat treated low-alloyed steel 42CrMo4 and austenitic stainless steel X6CrNiMo18-10-2) by one-step flame spraying and fusing process. The microstructure of coatings and coating/substrate interface but also the effects of deposition technology on the heat-treated steel substrates which have frequently been used in practice were investigated. The influence of the sample size on the microstructure was also discussed. A proof is given of the change in the structure of coating, coating/substrate interface and substrate due to high fusing temperature, depending on type of steel substrate (and relating thermal properties), coating thickness but also on dimensions of the sample.

ARTICLE HISTORY
Received 26 July 2016
Accepted 31 October 2016

KEYWORDS
Ni-based self-fluxing alloy coatings; flame spraying; SEM; EDS; microstructure; steel

1. Introduction

Ni-based self-fluxing alloy coatings are widely used under conditions of wear and corrosion and at increased temperatures. They contain B and Si that act (as well as Cr [1]) on decreasing melting temperature of pure nickel. B and Si improve fluxing (or fluidity, according to some authors) and wettability during deposition and also act as deoxidators, by forming borosilicate $B_2O_x{\cdot}SiO_y$ protecting other elements from oxidation [2]. However, in addition to the positive effect of these two elements, the presence of B and Si can make the process of crystallization more difficult [3]. It is pointed out that crystallization is also affected by molten particles' cooling rate on the substrate surface (at higher rates of cooling there is no time for crystallization and amorphous structures are formed) [3]. Addition of Cr to Ni-based self-fluxing alloys results in good resistance to corrosion, and due to the addition of C carbides are formed which along with borides, silicides, carboborides and some other phases in Ni matrix, affect the increase of hardness. However, the authors [4] who dealt with flame and laser spraying in their paper, claim that the addition of Cr, Fe and C in NiBSi alloy

CONTACT Katica Simunovic katica.simunovic@sfsb.hr

causes brittleness of the coating (decrease of toughness), along with the possible appearance of microcracks and without any significant improvement of hardness in the binder phase.

Ni-based self-fluxing alloy coatings are most often deposited by high velocity oxygen/air fuel spraying (HVOF, HVAF), flame (gas) low velocity spraying (LVOF), plasma spraying, laser cladding and plasma transferred arc welding (PTA or PTAW). The process of remelting (melting, fusing) is frequently and almost obligatorily applied subsequent to (or simultaneously with) the flame, HVOF and plasma spraying, because these alloys have originally been developed for the application in sprayed and fused state. According to [5,6], steel substrates were mostly used.

As to the structure of Ni-based self-fluxing alloy coatings, it is most often the case of matrix with dendritic γ Ni solid solution with Fe and Cr, with eutectics (for example Ni–Ni_3B and Ni_5Si_2 or Ni_3Si_2). The following phases were mentioned: Ni-8.64W–3.53C–3.03Si–3.59B and Ni–11.0B–0.43Si (flame spraying) then Ni–15.59W–2.13B–1.39Si–2.63C and Ni–9.29B–1.11Si (laser spraying), where there are W and C in the matrix due to dissolution of WC/W_2C hard particles during deposition [4]. Phases Ni–11.0B–0.43Si and Ni–9.29B–1.11Si provide toughness to coatings [4]. In depositing an Ni-based self-fluxing alloy coating, during deposition, in addition to the molten particles, partly molten but also unmolten particles of the powder can participate, as well as the particles hardened even before the contact with the substrate, due to a very high cooling rate [7]. Regular crystal structures can emerge but also amorphous phases. Thus, the amorphous phases were not observed in coatings deposited by flame spraying because the crystallization due to the lower cooling rate was made possible as the thicker molten droplets were involved (lower speed of particles and higher temperatures) [3]. In other words, with thicker splats on the substrate surface, cooling rate is lower and the crystallization process can begin. However, the evidence is given, even for the HVOF process, of the existence of crystal structure regardless of the highest rates of in-flight particles so that both the high cooling rates and amorphous structure were to be expected [3]. It is explained by higher temperature of substrate during the HVOF process as this temperature affected the molten splat lower rate of cooling and development of crystallization process [3]. In investigation [8] in which flame spraying and post heat treatment in furnace is analysed, the authors prove that segregation occurred due to different thickness of phases, i.e. a uniform distribution of phases in a coating did not exist.

Investigators mention different phases, mostly carbides and borides, but also carbo-borides and silicides (for example $(Cr, Fe)_7C_3$, $(Cr, Fe)_{23}C_6$, Cr_7C_2, Cr_7C_3, Cr_3C_2, $Cr_{23}C_6$, $(Fe, Ni)_{23}C_6$, Ni_2W_4C, $Fe_{23}(C, B)_6$, CrB, Fe_2B, Cr_2B, Ni_4B_3, (Ni, W)B, NiB, NiO, $NiCr_2O_4$, NiWSi, $Ni_{31}Si_{12}$, NiSi, $CeNi_2$, La_2Ni_3, La_2Ni, $Ce_3Ni_6Si_2$, $CeNi_{22}C_3$), whose occurrence, size and distribution as well as form can depend on chemical composition of Ni-based self-fluxing alloy, type and parameters of deposition technology, the same as on type and parameters of post spray treatment. Needle-like precipitates often appear in the structure [9–11], but the round shaped ones as well (for example in laser cladded coatings investigated in [9]). The addition of rare earth oxide can be of influence in preventing the formation of needle-like precipitate because the rare earth oxides segregate on grain boundaries (grains become cubic instead of needle-shaped) [10]. G/R ratio (where G is the actual temperature gradient ahead of the solid/liquid metal interface, and R is growth rate) mentioned in the research [12] is given as a factor of influence on the structure (dendritic structure for lower G/R ratio, planar or cellular structure for higher G/R ratios).

The authors [13] investigate and compare the structure of as-sprayed and sprayed and furnace melted coating at 1,073.15 K (800 °C) nearer to and further away from the coating/surface interface. They mention, for as-sprayed state, a black zone in the substrate near the coating/substrate interface and they claim that it was formed due to the segregation of carbon. The authors [14], who applied flame and fuse process, also mention a zone of 0.05–0.1 mm thickness with 700 HV0.1 microhardness. This is a zone in hardened and tempered substrate 42CrMo4, under the coating/substrate interface, into which carbon is segregated and higher hardness is measured. For as-sprayed and sprayed and melted state, the authors [13] compare also the amount of primary carbide and eutectic as well as the magnitude of carbide particles in the coating nearer to or further away from the coating/surface interface. For both states the carbide particles were less close to the coating/substrate interface and their amount was smaller. Comparison of both states, subsequent to the sprayed coating heat treatment, showed that the primary carbides amount was reduced while that of eutectics was increased.

In the paper [9], the authors think that the diffusion of Fe occurred from steel substrate into coating material. The same was also proven by the authors [15], who think that the diffusion of Fe (even up to 60 wt%) occurred due to small thickness of the coating and too powerful laser used for remelting. These authors also say that this is detrimental to corrosion persistence (along with microcracks) due to the tolerance being only 5–10 wt% of Fe. The authors [16] quote in their investigation that Ni and Cr diffused from the coating into the substrate, and that Fe dissolved into the liquid Ni-based alloy coating. In the paper [7] it is demonstrated that diffusion of elements between coating and substrate did not take place due to the lack of time (regardless of the as-sprayed coatings being subsequently flame treated).

Finally, the analysis of the most common substrates used in the investigations revealed that the steel substrates are most used by researchers [5,6], but the problem is that investigations dealing with potential influence of flame spraying and fusing process on previously heat treated steel substrates are rare. In fact, in practice, the coatings are often deposited on hardened (quenched) and tempered machine parts. So, in this study, one-step flame spraying and fusing process of depositing NiCrBSi coatings on steel substrates (two types were heat treated prior spraying) was applied. The microstructure of coating, coating/substrate interface and substrate was investigated. Moreover, the potential influence of the samples' dimensions on the microstructure was taken into consideration.

2. Experimental details

2.1. Coating material

Three types of NiCrBSi powder are applied, NiCrBSi (15 wt% Cr; 3.2 wt% B; 4.4 wt% Si; 0.7 wt% Fe; 0.7 wt% C; Ni balanced), NiCrWBSi (15 wt% Cr; 3 wt% B; 4 wt% Si; 3.5 wt% Fe; 0.8 wt% C; 17.3 wt% W; Ni balanced) and composite NiCrBSi powder with mechanically added WC hard particles (matrix 7 wt% Cr; 3 wt% B; 4.5 wt% Si; 5.8 wt% Fe; 0.1 wt% C; Ni balanced, and 60 wt% of WC). Different from the last mentioned composite powder, NiCrWBSi powder also contains WC, but in the form of fine phases uniformly dispersed in NiCrBSi particle of the powder [17,18]. Hard phases in this alloy precipitate during powder production, thus they are constituent parts of the powder and are not added

subsequently as with conventional composite powders. These powders were produced by the dry inert gas atomisation process using the nitrogen [19]. In this way, the powders with less oxidation than air, steam or water atomised powders and better spherodisation can be produced with uniform particle shape because of freezing the spray within an inert gas [19]. Accordingly, these powders are called micropowders or microflo fusible powders with very small particle size (from less than 25 to 140 μm). As to the WC grains in NiCrBSi + WC powder, it is about angular cast and crushed tungsten carbide particles [20] of up to 50 μm size.

2.2. Substrate material

Three types of steel substrate are applied, carbon steel C45 with 0.5 wt% carbon, low-alloyed steel 42CrMo4 with 0.43 wt% C, 1.18 wt% Cr and 0.3 wt% Mo and austenitic stainless steel X6CrNiMo18-10-2 with 0.04 wt% C, 17.8 wt% Cr, 10.72 wt% Ni and 2.48 wt% Mo. Substrate materials (steels) are marked according to the chemical composition (the norm EN 10027). First two steels, C45 and 42CrMo4 are hardened at 1,113.15 K (840 °C)/15 min, then water (C45) or oil (42CrMo4) quenched and tempered at 873.15 K (600 °C)/30 min. Structure of carbon steel C45 and low-alloyed steel 42CrMo4 subsequent to heat treatment was tempered martensite with average hardness 320 HV30 (30.3 HRC) and 400 HV30 (34.7 HRC), respectively, while the structure of stainless steel X6CrNiMo18-10-2 was austenitic with 202 HV30 hardness [14].

For depositing of coatings, samples with dimensions 75 × 25 × 12.5 mm were used, which are standard samples for dry sand/rubber wheel abrasion resistance test (according to ASTM G65 – Standard Test Method for Measuring Abrasion using the Dry Sand/Rubber Wheel Apparatus) and samples with dimensions 18 × 18 × 18 mm otherwise intended for testing solid particle erosion (schematic representation is given in Figure 1). Samples were ground before spraying and fusing in order to eliminate impurities, grease and oxides.

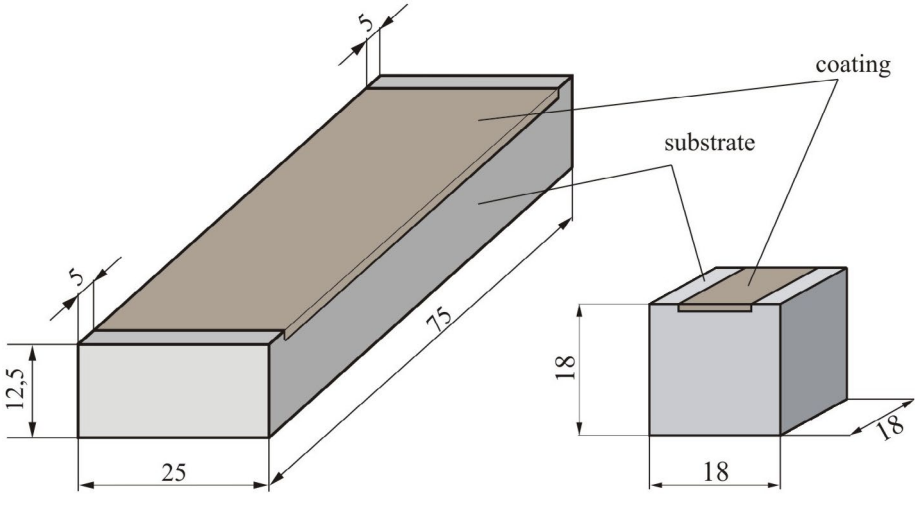

Figure 1. (colour online) Samples used for spray and fuse.

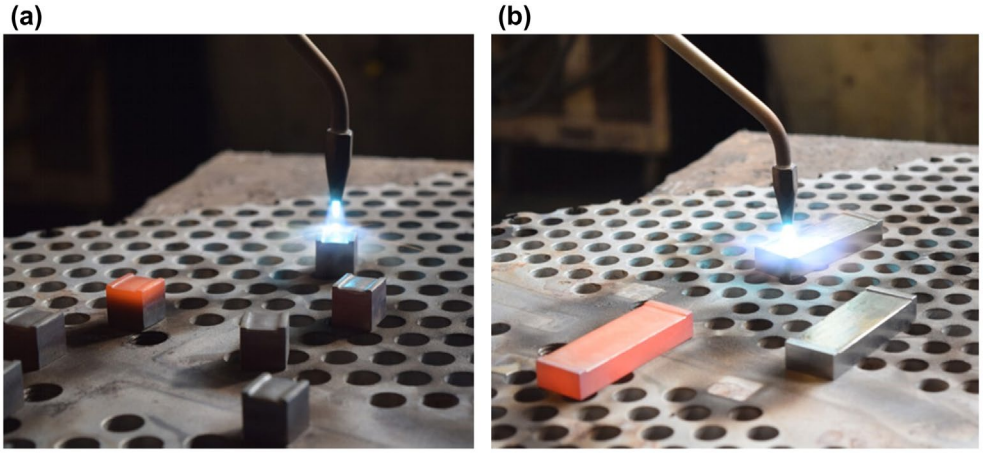

Figure 2. (colour online) Spraying and fusing by the use of (a) small and (b) big samples.

2.3. Deposition technology

The coatings were deposited by Eutalloy® one-step powder flame spraying and fusing process. Eutalloy® one-step powder flame spraying and fusing process (also applied in [21] where the authors use the term powder welding method for this process) is Castolin trade mark where alloy powders are sprayed onto the part to be coated and are fused simultaneously. Bonding is achieved by diffusion of the alloys into the substrate material without dilution [19]. Two different types of samples (schematically presented in Figure 1) during the flame spraying and fusing are shown in Figure 2. It is visible that the small sample did not have to be completely warmed up (to achieve the fusing temperature) because of concentrated heat input (where the torch practically did not have to move). Just contrary, to achieve and retain the fusing temperature, the complete warming up of bigger sample had to be done.

Acetylene pressure was 50,000 Pa, oxygen pressure 200,000 Pa. Subsequent to flame spraying and fusing and cooling in the air, samples were ground by a diamond grinder and cooled/lubricated simultaneously.

2.4. Metallographic preparation

To characterise the microstructure of coating, coating/substrate interface and substrate the samples of dimensions 75 × 25 × 12.5 mm were cut to size, where the small samples of 18 × 18 × 18 mm were used in its original size. Then the samples were ground, polished and etched. Grinding was performed, consecutively, by the use of 240, 600, 800 and 1,200 abrasive sheets. Fine polishing was performed by the use of 0.05 μm Al_2O_3 water suspension.

2.5. Microstructural analysis

Out of the nine coating/substrate combinations (Table 1), the three combinations (C45 steel substrate – NiCrBSi coating; 42CrMo4 steel substrate – NiCrBSi + WC coating and X6CrNiMo18-10-2 steel substrate – NiCrWBSi coating) were preliminary investigated by the use of light optical microscopy in [14], while in the present study, additional combinations

Table 1. Combinations of substrate and coating material.

Substrate material	Coating material	Coating thickness, mm
Carbon steel C45, heat treated before spraying and fusing	NiCrBSi	0.3
	NiCrBSi + WC	0.5
	NiCrWBSi	0.8
Low alloyed steel 42CrMo4, heat treated before spraying and fusing	NiCrBSi	0.5
	NiCrBSi + WC	0.8
	NiCrWBSi	0.3
Austenitic stainless steel X6CrNiMo18-10-2	NiCrBSi	0.8
	NiCrBSi + WC	0.3
	NiCrWBSi	0.5

were investigated. Scanning electron microscope/energy-dispersive spectrometer (SEM/EDS) analysis coupled by the light microscopy is used to prove some previous conclusions and draw additional conclusions regarding a particular combination of coating and substrate. Two replicates are applied for each coating/substrate combination to draw conclusions about the sample size influence on the microstructure but also for the possibility to use different etchants.

Therefore, for microstructural analysis cross section of each sample was metallographically prepared by grinding and polishing (as it is described in Section 2.4) and etched in nital or Adler solution, depending on the substrate, as well as in glyceregia (to reveal the microstructure of the coatings). Firstly, microstructure was observed under light microscope Olympus GX51 equipped with digital camera and then microstructure was analysed in detail by means of SEM Tescan Vega TS 5130 LS and Bruker's EDS with Quantax 200 software. The EDS analysis was performed in point. Also, mapping analysis, i.e. distribution of elements in default area was conducted.

3. Results

In this section, a detailed analysis of the microstructure of Ni-based self-fluxing alloys deposited on the steel substrates was presented, following the order of coating/substrate combinations from Table 1.

3.1. C45 steel substrate and coatings

Figure 3 shows the SEM micrographs of the cross sectioned sample of the hardened and tempered C45 steel substrate coated by NiCrBSi alloy (0.3 mm), etched in nital solution. Fine pearlite and ferrite grains remote from the coating can be clearly seen on the SEM micrograph (Figure 3(a)); it is proven that spraying and fusion conditions caused transformation of originally martensitic C45 steel [14] to the pearlite-ferritic microstructure. In accordance with EDS results, Figure 3(b) shows that in spot 1 besides elements from coating, there is a large amount of Fe (45.31 wt%). This could be explained by its diffusion from the substrate to coating. A commonly mentioned diffusion zone exists between the coating and substrate, which is mainly white coloured when using light microscopy. Further, in the microstructure of coating, Cr precipitates exist (spot 2). Also, EDS analysis showed a certain amount of chromium in the substrate which is probably due to its diffusion from coating.

In Figure 4 the microstructure of the cross sectioned sample of the hardened and tempered C45 steel substrate coated by NiCrBSi + WC (0.5 mm), etched in nital solution and

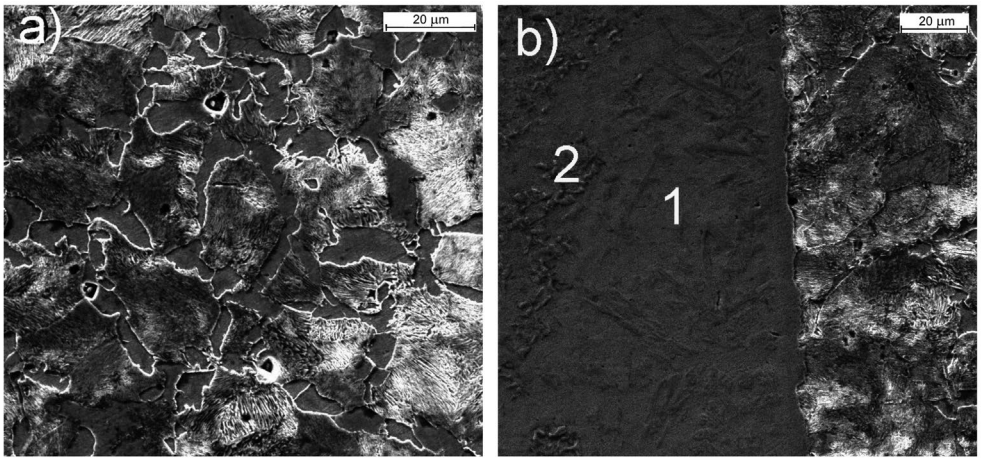

Figure 3. SEM micrographs for sample C45 steel substrate – NiCrBSi coating, (a) substrate and (b) coating/substrate interface.

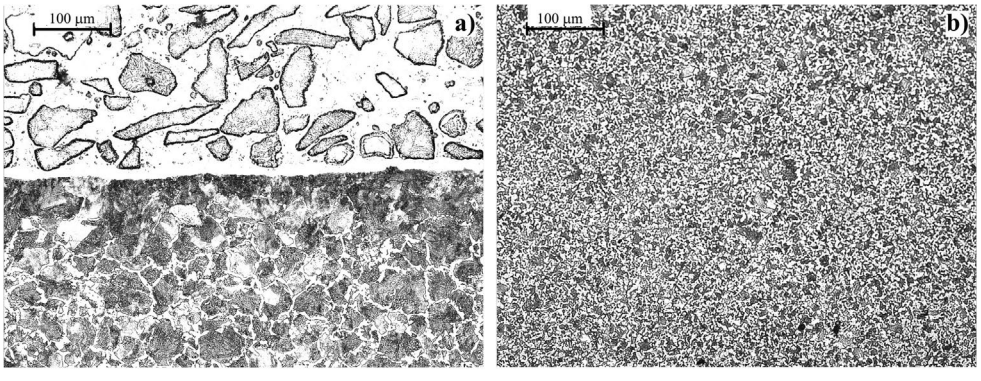

Figure 4. Light micrographs for sample C45 steel substrate – NiCrBSi + WC coating, (a) coating/substrate interface and (b) substrate.

observed by light microscope is shown. Two zones are visible: white zone of coating with uniformly distributed coarse grains of WC particles and dark zone of substrate. A thin white boundary between coating and substrate can be seen too. Grains of substrate are coarser under the coating/substrate interface (Figure 4(a)) than remote from the interface (Figure 4(b)). Coating/substrate interface of sample C45 steel substrate – NiCrBSi + WC coating analysed by SEM and EDS is shown in Figure 5(a). The microstructure of substrate is also transformed from martensitic to the pearlite-ferritic (Figure 5(b)). Carbon content in spot 1, Figure 5(a), is 1.18 wt%, in spot 2 is 1.21 wt% and 2.64 wt% in spot 3. These results of EDS analysis in point indicate that carbon content is the lowest in the coating/substrate interface. Results of EDS analysis in point also show that chemical composition of coarse grains in the coating microstructure corresponds to the tungsten carbides (WC). This is confirmed by the EDS mapping analysis which is presented in Figure 6. The above results of EDS point analysis that carbon content is the lowest in the coating/substrate interface can be seen in EDS mapping elements distribution (Figure 6).

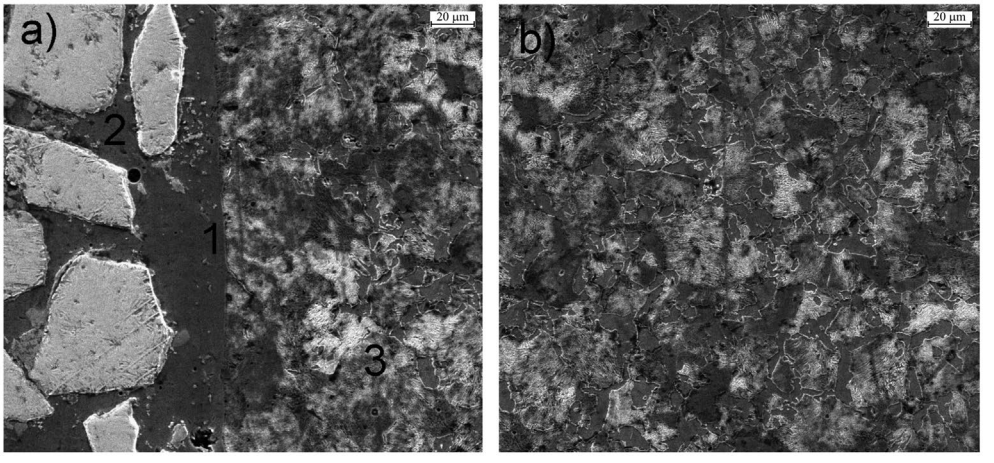

Figure 5. SEM micrographs for sample C45 steel substrate – NiCrBSi + WC coating, (a) coating/substrate interface and (b) substrate under the coating.

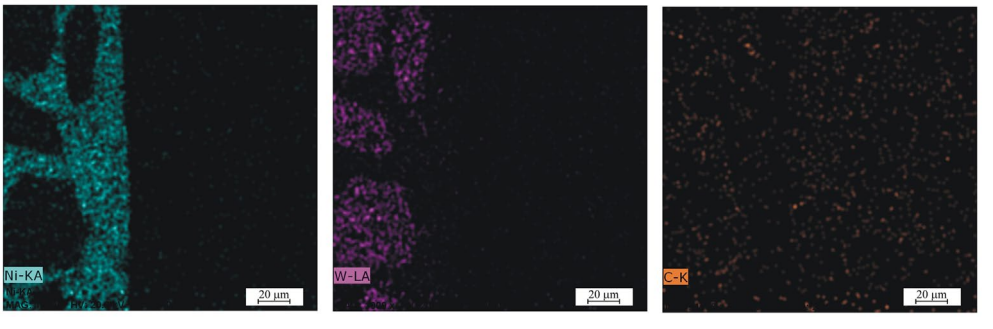

Figure 6. (colour online) EDS mapping analysis of sample C45 steel substrate – NiCrBSi + WC coating.

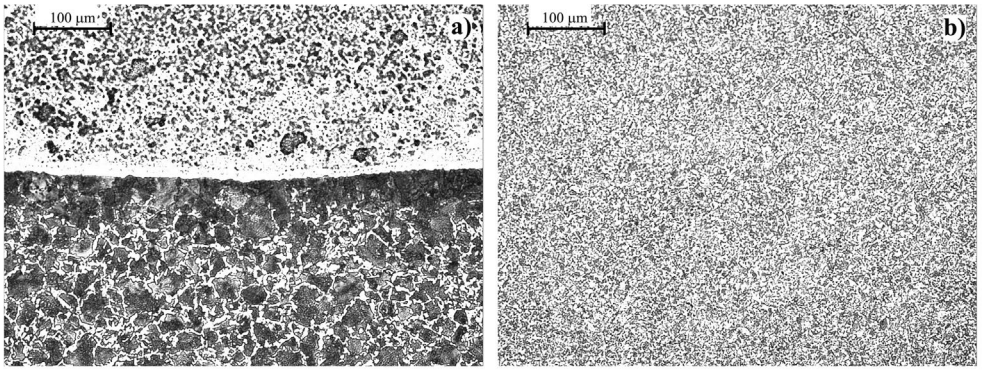

Figure 7. Light micrographs for sample C45 steel substrate – NiCrWBSi coating, (a) coating/substrate interface and (b) substrate.

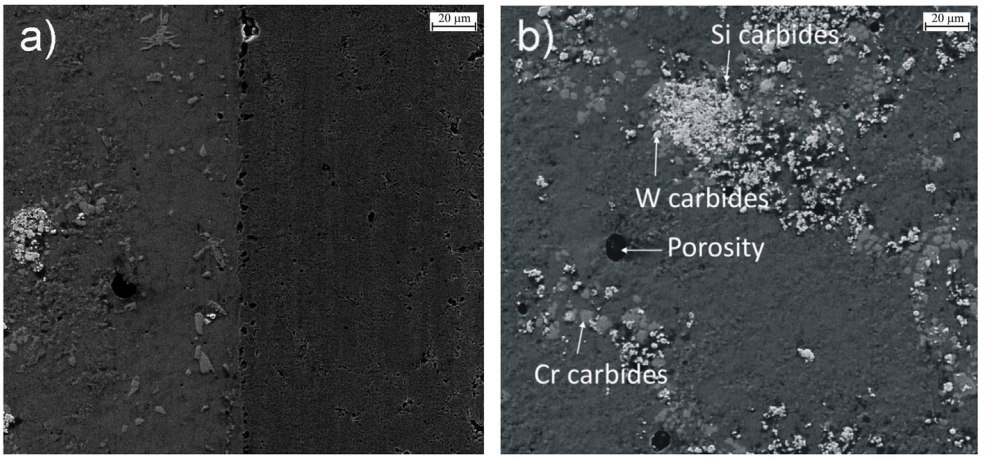

Figure 8. (colour online) SEM micrographs for sample C45 steel substrate – NiCrWBSi coating, (a) coating/substrate interface and (b) coating.

Microstructure of cross sectioned sample C45 steel substrate coated by NiCrWBSi, 0.8 mm is shown in Figure 7. Two zones are visible: white zone of coating and dark zone of substrate with an intermediate thin diffusion zone. Coarse grains are present under the coating/substrate interface, while finer grains are remote in the substrate. The dark zone under the coating can be caused by the carbon segregation (as it is also noticed by [13]). Figure 7(b) shows pearlitic-ferritic microstructure of substrate with finer grains of pearlite and ferrite. Micrographs of sample C45 steel substrate with NiCrWBSi coating obtained by SEM are presented in Figure 8. In Figure 8(a) coating/substrate interface can be seen. The EDS analysis in point showed that carbon content in coating is 2.08 wt%, in the coating/substrate interface is 1.87 wt% and in substrate is 2.23 wt%. These results indicate that carbon content is the lowest in the coating/substrate interface. Content of Fe in the coating is only 9.77 wt% meaning that there was negligible Fe diffusion from substrate to coating. According to EDS results, white rounded precipitates in Figure 8(b) corresponds to the tungsten and silicon carbides. Further, grey elongated precipitates visible in the coating/substrate interface (Figure 8(a)) present nickel borides, probably Ni_3B, while grey rounded and smaller nickel and chromium precipitates exist in the coating (Figure 8(b)).

3.2. 42CrMo4 steel substrate and coatings

Figure 9(a) shows microstructure of the cross sectioned sample 42CrMo4 steel substrate with NiCrBSi coating (0.5 mm). Sample was etched in nital solution. In the white zone of coating a large amount of grey precipitates can be seen. Detailed analysis of the microstructure was realised by SEM (Figure 10). EDS analysis in point showed that chromium carbo-borides are present in the coating remote from the coating/substrate interface. Before spray deposition martensitic structure was achieved [14], and it is retained after spraying (Figure 10(b)).

Figure 11 shows microstructures of sample 42CrMo4 steel substrate with NiCrBSi + WC coating (0.8 mm). In Figure 11(a) the coating/substrate interface is presented (etched with glyceregia). The coarse particles dominate in the microstructure of coating and they are

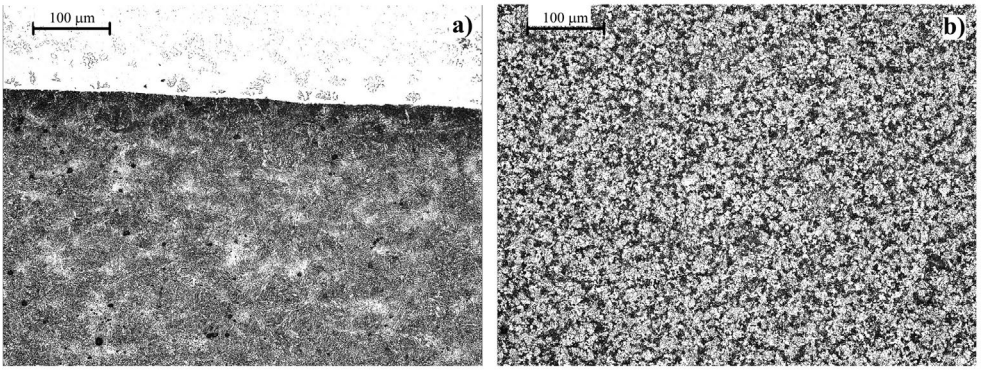

Figure 9. Light micrographs for sample 42CrMo4 steel substrate – NiCrBSi coating, (a) coating/substrate interface and (b) substrate.

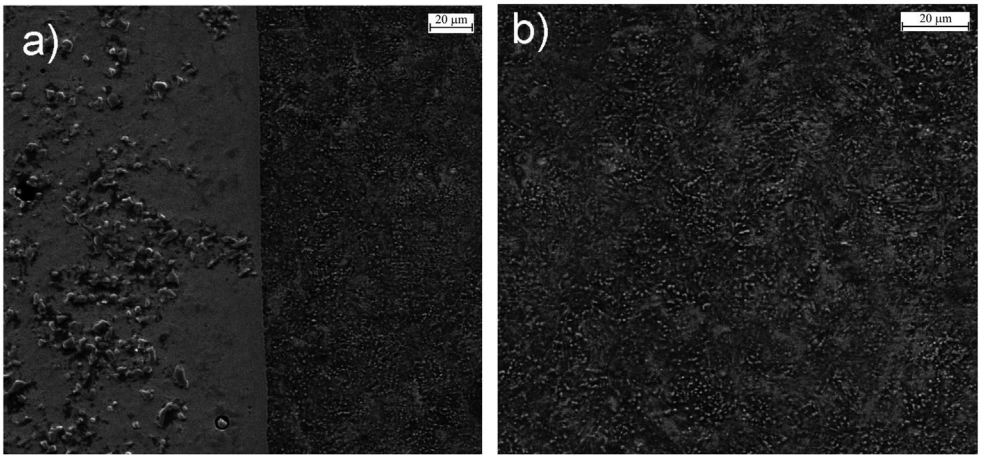

Figure 10. SEM micrographs for sample 42CrMo4 steel substrate – NiCrBSi coating, (a) coating/substrate interface and (b) substrate.

uniformly distributed. According to the EDS analysis results it is tungsten carbide (WC). The portion of nickel carbides and carboborides – probably Ni_7C_3, Ni_6(CB) (small light particles in the coating along the coating/substrate interface in Figure 11(a)), decreases with remoting from the coating/substrate interface. These particles distribution along the interface can be better seen in the sample etched in nital solution (Figure 12). The matrix of coating, area around the WC particles, consists of lighter and smaller darker particles of irregular shape (Figure 11(b)). According to the EDS results, lighter particles consist of Ni, Si, Cr carbides and borides while darker particles consist of Si and Cr carbides and borides. The microstructure of the substrate of sample 42CrMo4 steel is martensitic meaning that the martensite retained after the spraying (Figures 11(a) and 12). Figure 12 shows that nital etching of 42CrMo4 steel substrate coated by NiCrBSi + WC did not result in the revealing of the microstructure of coating matrix. Only WC particles as well as nickel carbides and nickel carboborides are visible.

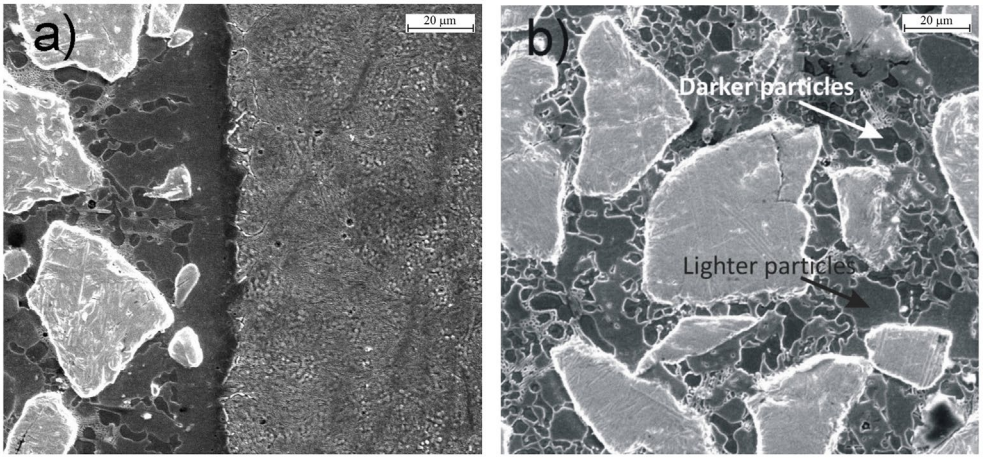

Figure 11. (colour online) SEM micrographs for sample 42CrMo4 steel substrate – NiCrBSi + WC coating, (a) coating/substrate interface and (b) coating (glyceregia).

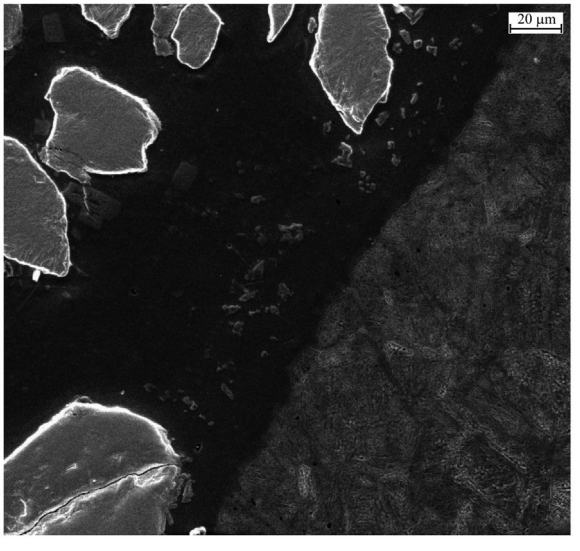

Figure 12. SEM micrograph for sample 42CrMo4 steel substrate – NiCrBSi + WC coating, coating/substrate interface (nital).

Microstructure of cross sectioned sample 42CrMo4 steel substrate with NiCrWBSi coating, 0.3 mm (nital) is presented in Figure 13. Figure 13(b) shows martensitic microstructure of the substrate which is retained after the spraying. The EDS results for sample 42CrMo4 steel substrate coated by NiCrWBSi show that carbon content in coating is 1.24 wt%, in the coating/substrate layer is 1.00 wt% and in substrate is 2.02 wt%. These results indicate that carbon content is the lowest in the coating/substrate interface. Content of Fe in the coating is 20.88 wt% indicating that diffusion of Fe from to substrate to coating occurred. White precipitates in the coating microstructure (Figure 13(a)) represent the tungsten and silicon carbides (WC, SiC), while chromium carbides and nickel carboborides are grey coloured.

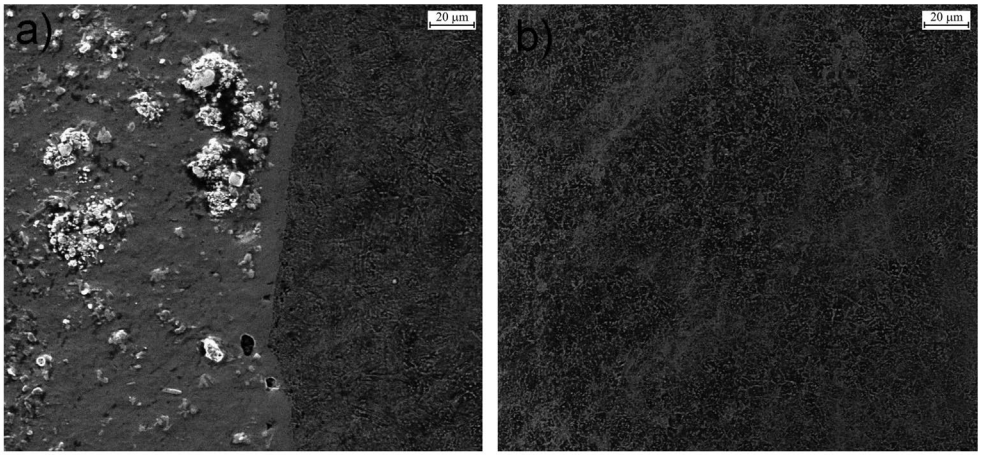

Figure 13. SEM micrographs for sample 42CrMo4 steel substrate – NiCrWBSi coating, (a) coating/substrate interface and (b) substrate.

3.3. X6CrNiMo18-10-2 steel substrate and coatings

Figure 14(a) shows light micrograph of sample X6CrNiMo18-10-2 steel substrate with NiCrBSi coating, 0.8 mm (Adler etchant). Two different zones can be seen: upper is coating and the bottom is austenite substrate. These two zones are split by coating/substrate interface below which austenitic grains are smaller than in matrix phase of substrate which can be clearly seen in SEM micrograph shown in Figure 14(b). Microstructure of NiCrBSi coating etched in glyceregia is presented in Figure 15(a), while the microstructure of substrate etched in Adler reagent is presented in Figure 15(b). Microstructure of substrate is fully austenitic (Figure 15(b)). Detailed microstructural analysis of this sample using the SEM and EDS showed that microstructure of the coating consists of Ni, Cr and Si carbides and borides which could be Ni_7C_3, $Cr_{23}C_6$, SiC, Ni_3B (Figure 15(a)). Further, the coating contains a certain amount of eutectic. Microstructure of coating matrix of sample 42CrMo4

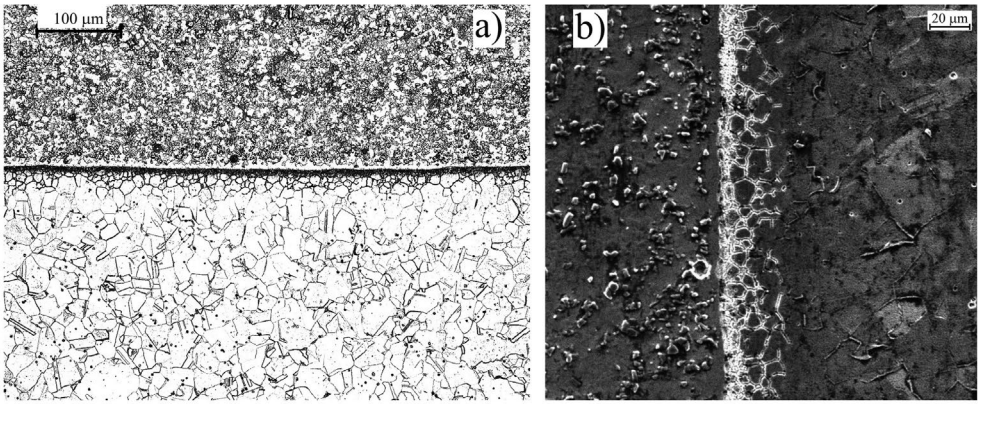

Figure 14. (a) Light and (b) SEM micrographs for coating/substrate interface of sample X6CrNiMo18-10-2 steel substrate – NiCrBSi coating.

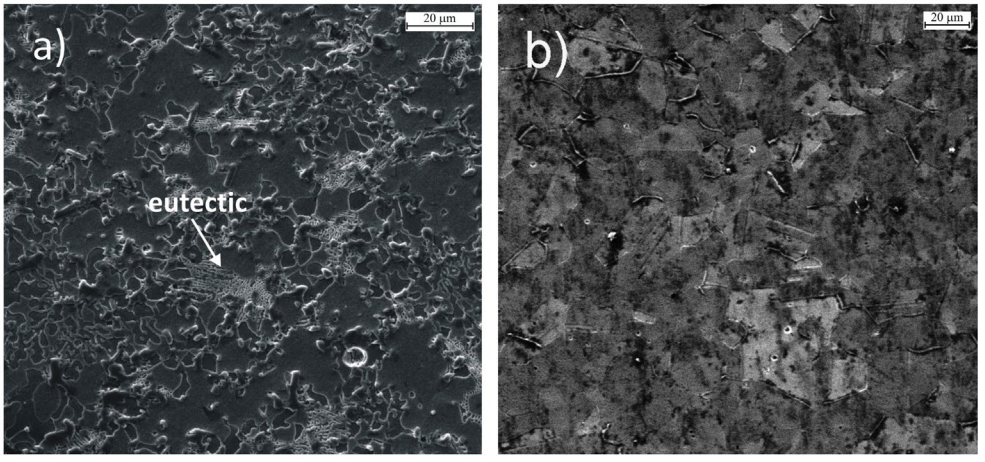

Figure 15. (colour online) SEM micrographs for (a) coating (glyceregia) and (b) substrate (Adler etchant) of sample X6CrNiMo18-10-2 steel substrate – NiCrBSi coating.

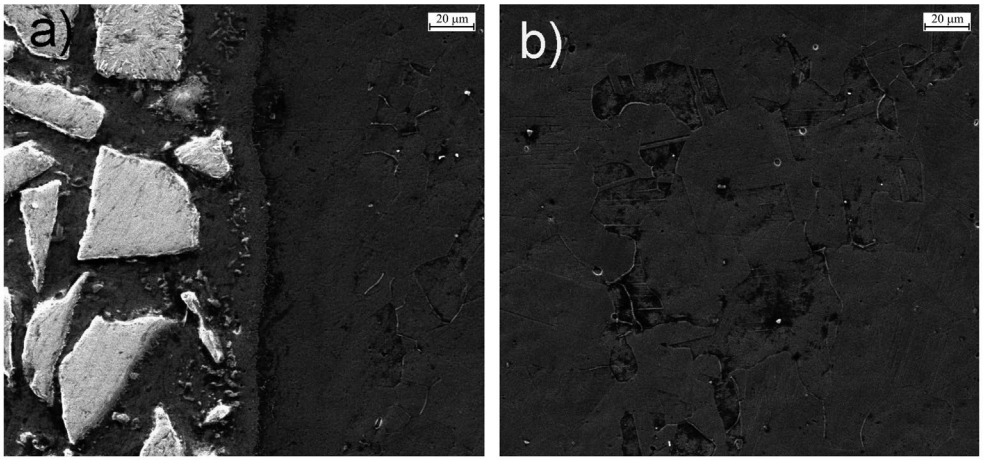

Figure 16. SEM micrographs for (a) coating/substrate interface and (b) substrate of sample X6CrNiMo18-10-2 steel substrate – NiCrBSi + WC coating.

steel substrate with NiCrBSi + WC coating (Figure 11(b)) is very similar to matrix of this sample. When comparing these two microstructures it can be seen that the microstructure of the coating matrix on the sample X6CrNiMo18-10-2 steel substrate (Figure 15(a)) is much finer than the coating matrix on the sample 42CrMo4 steel substrate (Figure 11(b)). The reason for this could be found in tungsten carbide content in coating powder deposited on the 42CrMo4 steel substrate.

Figure 16 shows SEM micrographs of coating/substrate interface and substrate of sample X6CrNiMo18-10-2 steel substrate with NiCrBSi + WC coating (0.3 mm) etched in Adler solution. It can be seen that uniformly distributed coarse (white) WC particles dominate in the microstructure of coating (Figure 16(a)). The results of chemical composition analysis in point by EDS showed that portion of Fe decreases when remoting from the substrate

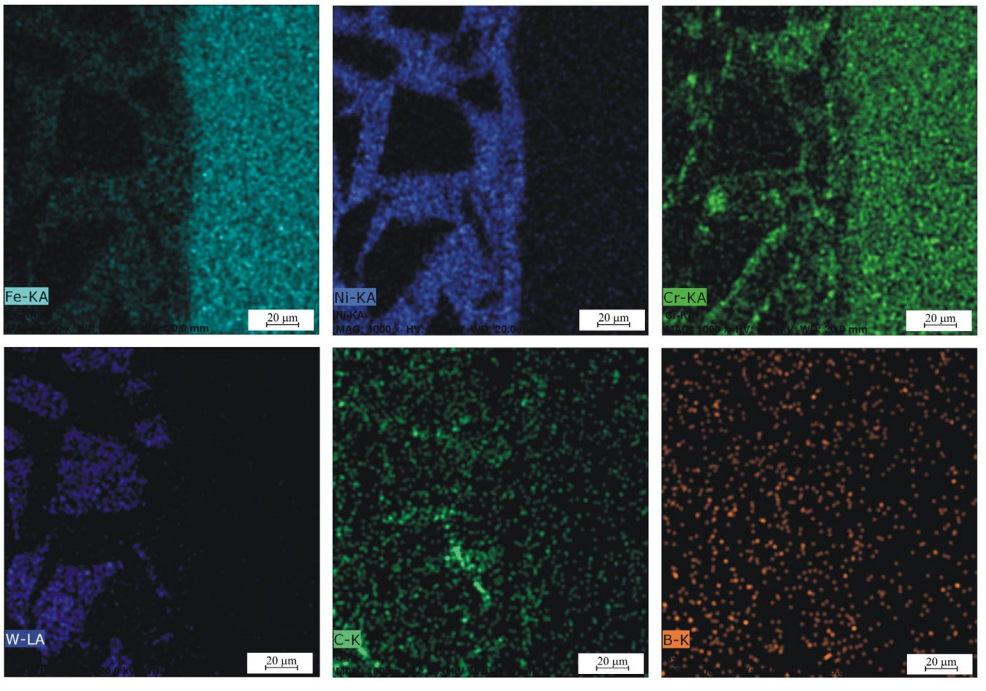

Figure 17. (colour online) EDS mapping analysis of sample X6CrNiMo18-10-2 steel substrate – NiCrBSi + WC coating.

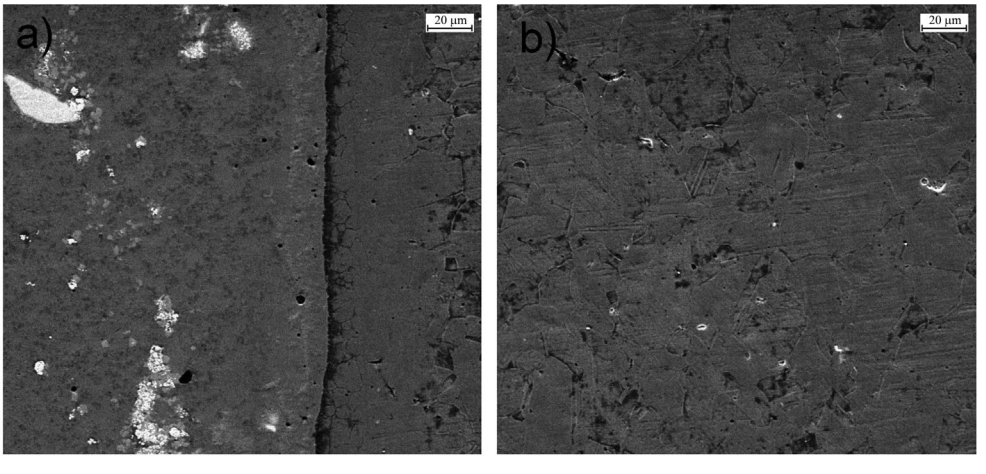

Figure 18. SEM micrographs for (a) coating/substrate interface and (b) substrate of sample X6CrNiMo18-10-2 steel substrate – NiCrWBSi coating.

(63.80 wt%) across the interface (21.83 wt%) to coating (8.74 wt%) which is confirmed by EDS mapping analysis (Figure 17). Figure 17 shows chemical elements distribution in the microstructure shown in Figure 16(a). It can be seen that around the WC, nickel and chromium borides as well as carbides are present. Further, it is obvious that diffusion of boron from coating to substrate occurred.

Figure 18 shows SEM micrographs of coating/substrate interface of sample X6CrNiMo18-10-2 steel substrate with NiCrWBSi coating, 0.5 mm (Adler etchant). According to the EDS analysis, microstructure of coating consists of Ni and Cr carbides and borides (dark particles) which could be Ni_3B, Cr_2B, Cr_7C_3 as well as small amount of tungsten and silicon precipitates – WC, SiC (white particles). Microstructure of substrate is austenitic and it is also confirmed that austenitic grains are smaller under the coating/substrate interface than in the substrate remote from the interface.

3.4. Influence of sample dimensions on microstructure

With the main aim to investigate the influence of the samples' dimensions on the microstructure, additional microstructural investigations are carried out by the use of the light microscope Leica DM 2500M. In this section, the accent is put on the substrate structure since the coating/substrate interface and coatings are analysed in previous subsections. For the sake of brevity, among all the 18 investigated samples and related micrographs, only some of figures are inserted.

Some preliminary conclusions can already be drawn from Figure 2 (Section 2.2) since it is visible that the small sample is not completely warmed up, while for the bigger sample the situation is just opposite. Therefore, the notable difference in the structure, especially for small samples, can be expected. For evidence, in Figure 19 one can notice that for the small samples the significant difference in the microstructure of the C45 steel substrate occurs at distance 2–5 mm from the coating, while for the samples cut from bigger ones it happens at distance 5–8 mm (or even more) from the coating. Actually for bigger sample substrate the structure is more uniform through the thickness because of full warming up (especially by increasing the coating thickness which requires more passes, i.e. prolonged heating). These conclusions are valid for all the combinations of three coatings and C45 steel substrate.

For all the combinations of three coatings and 42CrMo4 steel substrate the similar conclusions are valid as for the previous steel although the situation is not as clear and expected since the 42CrMo4 steel contains alloying elements. The microstructures of the 42CrMo4 substrate for the different samples' dimensions, but at the same distances from the coating are shown in Figure 20. It can be seen that there is also a difference between the structures at the same distances. Also, the significant change in structure is notable between 2 and 5 mm for the small sample, while the structure of bigger sample is uniform through the thickness.

When considering the combinations of substrate X6CrNiMo18-10-2 with all three coatings, again the structure of the sample cut from bigger sample substrate is uniform through the thickness, with no doubt. For the small samples coated with NiCrBSi + WC and NiCrWBSi (the thicknesses of 0.3 and 0.5 mm, respectively), the considerable change in structure is noticed again at distances from 2 to 5 mm where coarse grains change to fine ones. For the small sample but coated with NiCrBSi coating of 0.8 mm thickness, the appearance of coarse grains is not noticed (compare the structures of small substrate at the same distance but coated with different coatings of different thicknesses, Figure 21). So, the conclusion can also be drawn, that the coating thickness can have the additional influence on the microstructure of the substrate because for the thicker coating more passes have to be performed. In this way, some interaction between the dimension of the sample and coating thickness can exist.

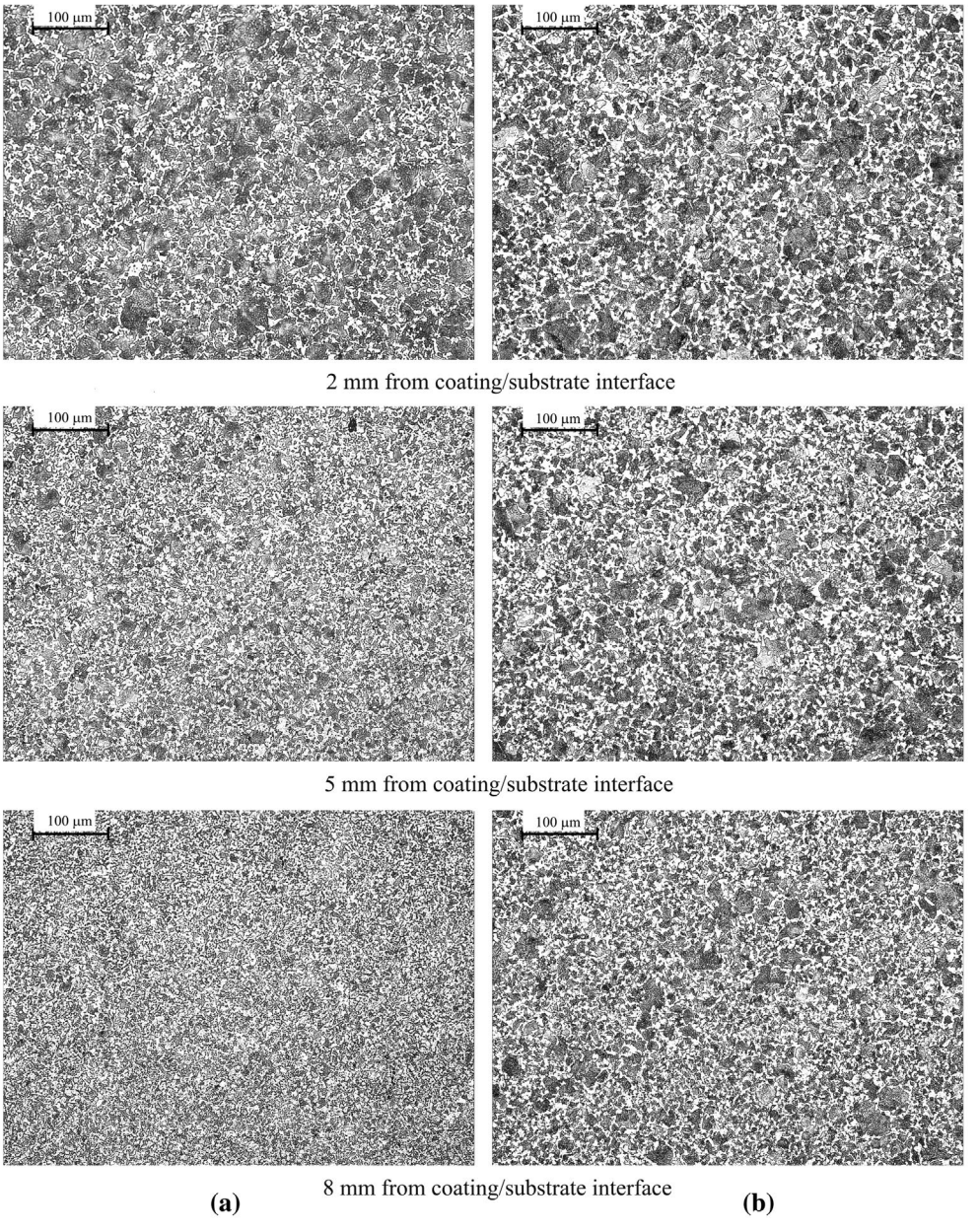

Figure 19. Microstructure of C45 substrate coated by 0.8 mm thick NiCrWBSi coating, (a) small sample and (b) sample cut from bigger sample.

When considering the influence of the sample dimension on the structure of coating, no considerable change was noticed for the 18 samples, except from the combination of NiCrBSi coating/C45 steel. There is a clear difference in NiCrBSi coating structure (of 0.3 mm thickness) on small and big C45 substrate sample (Figure 22). The occurrence of dendritic structure in the coating near the substrate is noticed for the small sample, while the uniform precipitate structure is revealed for the bigger sample. It can be explained by

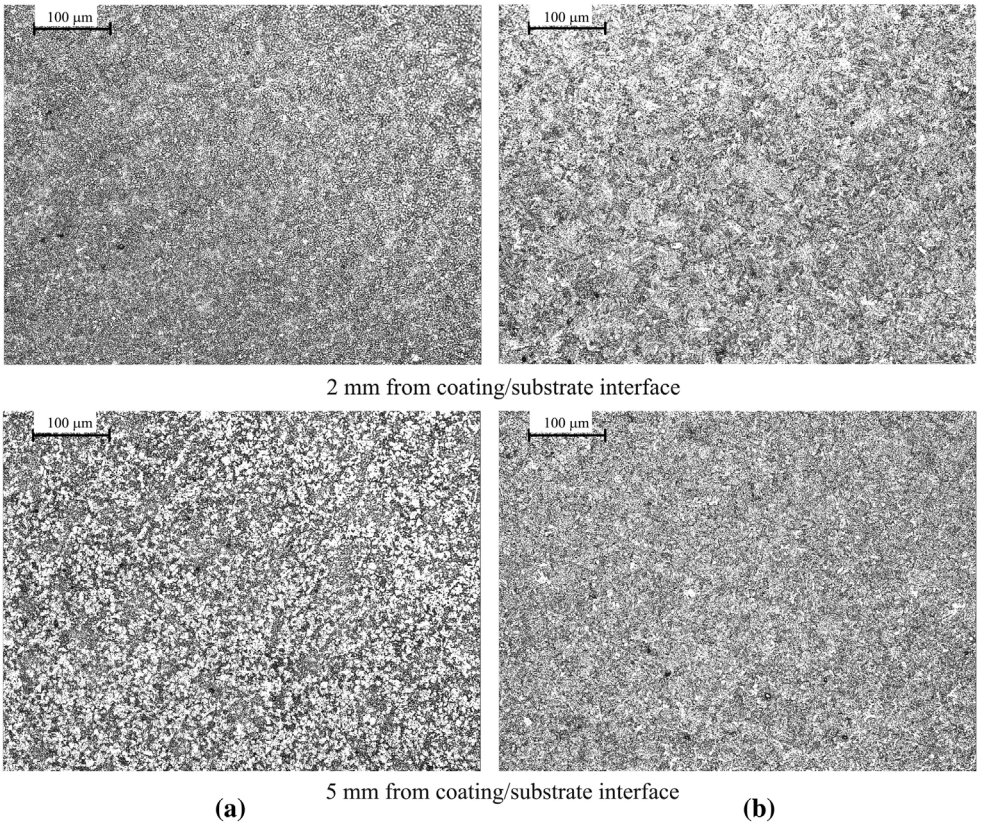

Figure 20. Microstructure of 42CrMo4 substrate coated by 0.8 mm thick NiCrBSi + WC coating, (a) small sample and (b) sample cut from bigger sample.

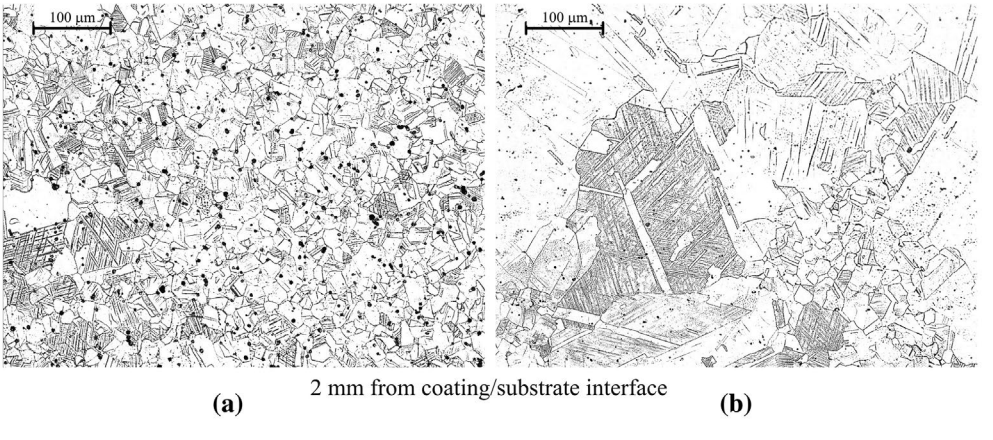

Figure 21. Microstructure of X6CrNiMo18-10-2 small sample substrate coated by (a) NiCrBSi coating of 0.8 mm thickness and (b) NiCrWBSi coating of 0.5 mm thickness.

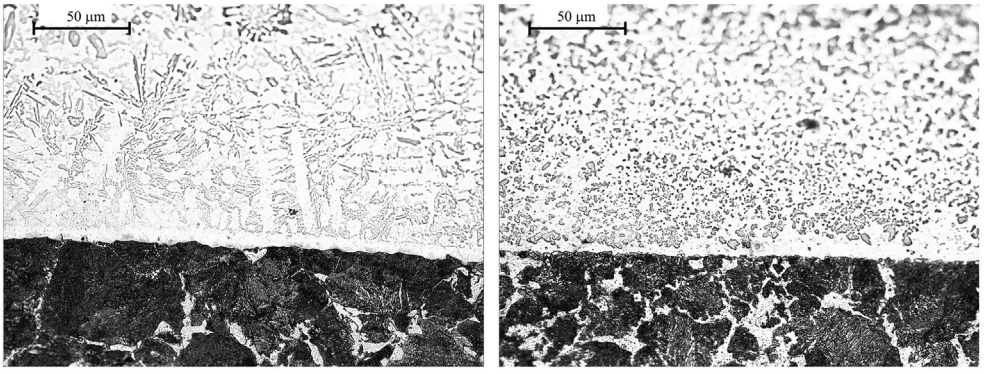

Figure 22. Microstructure of 0.3 mm thick NiCrBSi coating on C45 substrate, (a) small sample and (b) sample cut from bigger sample.

shorter heating time for small sample and the thinnest coating and, consequently, by faster cooling. Thus, the dendritic structure similar to casting appeared.

4. Discussion

According to the above analysis, the discussion comprising the comparison of the coatings' microstructure and the influence of high fusing temperature on the substrate structure is presented.

For NiCrBSi coating a higher amount of excreted precipitates (chromium carbo-borides, Ni, Cr and Si carbides and borides, respectively) is characteristic. Precipitates are uniformly distributed across the thickness of NiCrBSi coating deposited on the X6CrNiMo18-10-2 steel substrate (0.8 mm thickness), whereas the deposition of this coating on the C45 and 42CrMo4 steel substrates resulted in a lower amount of precipitates close to the coating/substrate interface. This is probably due to a lower thickness of coating (0.3 and 0.5 mm, respectively) and consequently due to a shorter deposition time. This is more pronounced for small samples (with even shorter heating time and consequently faster cooling which resulted in formation of dendritic structure near coating/substrate interface (discussed in Section 3.4). Another reason for this could be found in a good thermal conductivity of unalloyed C45 and low alloyed 42CrMo4 steels (higher heat transfer rate) and therefore in a smaller amount of available thermal energy in the coating needed for the formation of precipitates along the substrate. For deposition of this NiCrBSi coating on the high-alloyed X6CrNiMo18-10-2 steel due to poor thermal conductivity of the substrate, there has been a higher amount of thermal energy in the coating for the formation of precipitates. Therefore they are present in the coating/substrate interface.

When comparing to NiCrBSi coating, in the NiCrWBSi coating there is a smaller amount of different precipitates; tungsten carbides occur and they are significantly smaller when compared to the mechanically added tungsten carbides in the NiCrBSi + WC coating. Microstructure of NiCrBSi coating is very similar to NiCrBSi + WC coating matrix, but is much finer which can be explained by the tungsten carbide content in coating powder NiCrBSi + WC. Also, nickel and chromium borides as well as carbides are present around

the WC particles. Eutectic is also found in both of coatings which is not the case for the NiCrWBSi coating.

For the smallest thickness of coatings (0.3 mm) it has been proven that in combination C45 steel substrate – NiCrBSi coating and 42CrMo4 steel substrate – NiCrWBSi coating diffusion of Fe from the substrate to the coating occurred (45.31 and 20.88 wt%, respectively). It would be in accordance with the conclusions in [15]. However, for the combination X6CrNiMo18-10-2 steel substrate – NiCrBSi + WC coating with the same coating thickness (0.3 mm) the situation is just opposite (only 8.74 wt% Fe is present in the coating) which could also be explained by the poor thermal conductivity of austenitic stainless steel. For the largest coating thickness (0.8 mm), for the combination C45 steel substrate – NiCrWBSi coating there was a small amount of Fe (only 9.77 wt%) in the coating meaning that diffusion of Fe from the substrate to the coating was negligible. Some authors claim that the thicker coatings allow more time for diffusion. The authors of this paper can state that it is not only about the thickness of the coating since in this investigation it is proven that there are different amounts of Fe in the coating regardless the coating thickness. The type of the substrate (having in mind the deposition technology and fusion treatment) can also affect the diffusion as it is proved in this paper.

For the C45 steel substrate, for all the combinations and independently on sample size, it may be concluded that under the coating dark zone exists, probably due to the carbon segregation. Also, grains of substrate are coarser under the coating/substrate interface (heat affected zone) and the microstructure of substrate is transformed from originally martensitic (prior to spraying and fusing) to the pearlite-ferritic structure (after the depositing). C45 is unalloyed carbon steel, and the conditions of spraying and fusing (temperature above 1,000 °C) and subsequent slow cooling affected the formation of pearlite and ferrite. Contrary to the C45 steel, in the heat affected zone of austenitic stainless steel X6CrNiMo18-10-2, smaller austenitic grains than in matrix of substrate were occurred because the temperature of fusing caused the hardening of austenitic stainless steel (these steels harden from temperature of 1,020–1,120 °C which is actually the temperature of fusing). The zone of fine grains is narrower for the small samples, because of shorter time of heating. For the low alloyed steel 42CrMo4, martensitic structure achieved before spray deposition was retained after spraying. The authors [22] who also applied heat treated 42CrMo4 steel as the substrate, concluded that after induction fusing of flame sprayed coatings, hardness of the substrate under the coating/substrate interface increased, due to the quenching effect (shorter fusing and cooling time). A similar conclusion is drawn in [14], but for flame fusing. Contrary to induction fusing and conclusions in [14], the authors [22] claim that flame fusing did not result by the substrate hardness increase. Changes in the substrate subsequent to furnace heat treatment and remelting of flame sprayed coatings are pointed out also by [1] who mentioned the detrimental reduction of hardness and decarburizing of the low carbon steel substrate. The authors [8] applied pure argon gas during heat treatment in the furnace, so as to prevent the high temperature oxidation and decarburization of the substrate. In the investigation [23] the authors noticed even three different zones after the HVOF process and laser remelting: pure coating layer with coarse precipitates, then intermediate coating layer with fine-grained precipitates, both of high and similar hardness, and finally dilution layer (with hardness higher than the substrate hardness and lower than the coating hardness). They also mention reduction of the substrate hardness with regard to as-sprayed state, due to annealing of grit blasting compressive stress during flame and laser remelting of HVOF sprayed coatings.

5. Conclusions

In the present paper, the nine combinations of substrate material (carbon steel, low and high alloyed steels) and coatings (NiCrBSi, NiCrBSi + WC and NiCrWBSi) obtained by one-step flame spraying and fusing are investigated. Below the conclusions about the coatings and substrates can be found.

Based on the above discussion it can be concluded that the microstructure of a particular coating obtained by the same processing parameters can be influenced by the substrate (the thermal conductivity) as well as the coating thickness since the diffusion time can be different. However, for making additional conclusions related to the coating thickness, further investigations may include, in addition to nine combinations of three coating materials and three materials of substrate, another 18 combinations in which all three thicknesses of coatings for each combination of coating and substrate would be involved.

Also, the results of this investigation prove that the high fusing temperature (about 1,100 °C) affects in a different way the structure of the steel substrate depending on the level of substrate alloying. Thus, the general opinion and statement that the high temperature of remelting has a great influence on substrate structure and properties, sometimes has to be modified (i.e. the substrate type has to be mentioned as well as the deposition technology and fusing treatment).

The influence of the sample dimensions on the microstructure should not be ignored since the different times of heating can significantly influence the microstructure of the substrate. When considering the real situation, the application of bigger samples can be a better simulation since the torch actually moves along the real workpiece.

Finally, the thermally sprayed coatings are far from thermodynamically balanced state (because of high rates of deposition and cooling), and therefore it is not surprising that some authors have drawn the different (even opposite) conclusions (but the true ones) for the similar situations.

Disclosure statement

No potential conflict of interest was reported by the authors.

References

[1] Z. Bergant and J. Grum, *Quality improvement of flame sprayed, heat treated, and remelted NiCrBSi coatings*, J. Therm. Spray Technol. 18 (2009), pp. 380–391.
[2] J.P. Tu, M.S. Liu, and Z.Y. Mao, *Erosion resistance of Ni-WC self-fluxing alloy coating at high temperature*, Wear 209 (1997), pp. 43–48.
[3] M.P. Planche, H. Liao, B. Normand, and C. Coddet, *Relationships between NiCrBSi particle characteristics and corresponding coating properties using different thermal spraying processes*, Surf. Coat. Technol. 200 (2005), pp. 2465–2473.
[4] A. Sue, H. Sreshta, and B.H. Qiu, *Improved hardfacing for drill bits and drilling tools*, J. Therm. Spray Technol. 20 (2011), pp. 372–377.
[5] K. Simunovic, T. Saric, and G. Simunovic, *Different approaches to the investigation and testing of the Ni-based self-fluxing alloy coatings-A review. Part 1: General facts, wear and corrosion investigations*, Tribol. Trans. 57 (2014), pp. 955–979.
[6] K. Simunovic, T. Saric, and G. Simunovic, *Different approaches to the investigation and testing of the Ni-based self-fluxing alloy coatings-A review. Part 2: Microstructure, adhesive strength, cracking behavior, and residual stresses investigations*, Tribol. Trans. 57 (2014), pp. 980–1000.

[7] D. Chaliampalias, G. Vourlias, E. Pavlidou, S. Skolianos, K. Chrissafis, and G. Stergioudis, *Comparative examination of the microstructure and high temperature oxidation performance of NiCrBSi flame sprayed and pack cementation coatings*, Appl. Surf. Sci. 255 (2009), pp. 3605–3612.
[8] Z. Bergant, U. Trdan, and J. Grum, *Effect of high-temperature furnace treatment on the microstructure and corrosion behavior of NiCrBSi flame-sprayed coatings*, Corros. Sci. 88 (2014), pp. 372–386.
[9] T. Gómez-del Río, M.A. Garrido, J.E. Fernández, M. Cadenas, and J. Rodríguez, *Influence of the deposition techniques on the mechanical properties and microstructure of NiCrBSi coatings*, J. Mater. Process. Technol. 204 (2008), pp. 304–312.
[10] Z. Zhang, Z. Wang, B. Liang, H.B. Dong, and S.V. Hainsworth, *Effect of CeO2 on the microstructure and wear behavior of thermal spray welded NiCrWRE coatings*, Wear 262 (2007), pp. 562–567.
[11] R. González, M.A. García, I. Peñuelas, M. Cadenas, M.D. Fernández, A.H. Battez, and D. Felgueroso, *Microstructural study of NiCrBSi coatings obtained by different processes*, Wear 263 (2007), pp. 619–624.
[12] B.M. Dhakar, D.K. Dwivedi, and S.P. Sharma, *Studies on remelting of tungsten carbide and rare earth modified nickel base alloy composite coating*, Surf. Eng. 28 (2012), pp. 73–80.
[13] S. Harsha, D.K. Dwivedi, and A. Agarwal, *Performance of flame sprayed Ni-WC coating under abrasive wear conditions*, J. Mater. Eng. Perform. 17 (2008), pp. 104–110.
[14] K. Simunovic, I. Kladaric, and D. Krumes, *Investigation of substrate microstructure after flame spraying and fusing*, Strojarstvo 50 (2008), pp. 213–220.
[15] J. Suutala, J. Tuominen, and P. Vuoristo, *Laser-assisted spraying and laser treatment of thermally sprayed coatings*, Surf. Coat. Technol. 201 (2006), pp. 1981–1987.
[16] Z. Zhang, Z. Wang, and B. Liang, *Microstructure and dry-sliding wear behavior of thermal sprayed and fused Ni-based coatings with the addition of* La_2O_3, Tribol. Lett. 37 (2010), pp. 141–148.
[17] L. Gil and M.H. Staia, *Microstructure and properties of HVOF thermal sprayed NiCrWBSi coatings*, Surf. Coat. Technol. 120–121 (1999), pp. 423–429.
[18] L. Gil and M.H. Staia, *Influence of HVOF parameters on the corrosion resistance of NiCrWBSi coatings*, Thin Solid Films 420–421 (2002), pp. 446–454.
[19] *Castolin Eutectic Global Coating Technology*. Available at https://www.castolin.com/sites/default/files/product/downloads//Global-Coating-Catalogue-2014.pdf (assessed on 25 August 2016).
[20] *Technical Data Book*. Available at http://www.ngoclinh.net.vn/sites/1637/upload/documents/2007_eutectic_data_book.pdf (assessed on 25 August 2016).
[21] N.Y. Sari and M. Yilmaz, *Improvement of wear resistance of wire drawing rolls with Cr-Ni-B-Si+WC thermal spraying powders*, Surf. Coat. Technol. 202 (2008), pp. 3136–3141.
[22] J. Voyer and H. Kreye, *Determination of cracking resistance of thermal spray coatings during four-point bend testing using an acoustic emission technique*, J. Therm. Spray Technol. 12 (2003), pp. 416–426.
[23] S. Houdková, E. Smazalová, M. Vostřák, and J. Schubert, *Properties of NiCrBSi coating, as sprayed and remelted by different technologies*, Surf. Coat. Technol. 253 (2014), pp. 14–26.